Menemui Matematik
(Discovering Mathematics)

journal homepage: https://persama.org.my/dismath/home

Bayesian Analysis of Longitudinal Data with Space-Time Interaction

Aliyu Abba Mustapha[1*], Hani Syahida Zulkafli[1], Jayanthi Arasan[1] and Jasse Faez Firdauss Abdullah[2]

[1] Department of Mathematics and Statistics, Universiti Putra Malaysia, 43400 UPM Serdang, Selangor, Malaysia.
[2] Department of Veterinary Clinical Studies, Universiti Putra Malaysia, 43400 UPM Serdang, Selangor, Malaysia.

[1]gs61204@student.upm.edu.my
[*]Corresponding author

Received: 2 January 2025
Accepted: 29 March 2025

ABSTRACT

This paper presents a Bayesian spatio-temporal model for longitudinal data-sets with covariates. The main aim is to develop a hierarchical spatio-temporal model that effectively integrates spatial random effects to account for unobserved spatial heterogeneity and autocorrelation, temporal random effects to capture dependencies and trends over time, and interaction terms to evaluate covariate relationships across space and time. By adding interaction terms, spatio-temporal models are significantly enhanced, enabling them to capture the complex interdependencies between variables across both spatial and temporal dimensions. This improvement allows for a more thorough analysis of the data, leading to deeper insights and more effective decision-making in practical applications. The use of a conditional autoregressive (CAR) prior is useful in handling the dependencies between neighbouring spatial units. The numerical results on simulated data illustrate the validity of the model.

Keywords: Spatio-temporal model, Spatio effect, Temporal effect, Interaction effect, Bayesian hierarchical model

INTRODUCTION

Spatio-temporal modelling is a useful approach for analyzing phenomena that show variations across both space and time [1]. Bayesian hierarchical binomial logistic regression offers a flexible framework that incorporates spatial, temporal, and space-time interaction effects, facilitating comprehensive analysis of binary outcomes [2].

In spatio-temporal models, the inclusion of space, time, and their interaction is essential for capturing the complex dynamics of the phenomenon being investigated [3]. The model utilizes spatial random effects to address unobserved spatial heterogeneity and spatial autocorrelation, temporal random effects to capture dependencies and trends over time, and interaction terms to assess how the relationship between covariates and binary outcomes varies across space and time [4].

The pioneering work of [5] introduced a Bayesian hierarchical spatiotemporal model for disease risk, accounting for both spatial and temporal effects along with their interaction. Subsequent studies have extended this approach to address specific challenges and improve computational efficiency. For example, [6] proposed using fixed rank kriging to handle large spatial datasets in spatiotemporal models.

With the growing availability of high-resolution spatio-temporal data, more sophisticated models have been developed. This has driven the advancement of new techniques and tools. Notably, Bayesian hierarchical modelling has become popular due to its ability to incorporate uncertainty and variability at multiple levels of the model [7].

Bayesian hierarchical binomial logistic regression, which integrates spatial, temporal, and space-time interaction effects, has wide-ranging applications across various fields. For example, [8] used this approach to study infectious disease counts, examining the spatial, temporal, and spatio-temporal patterns of disease transmission.

The goals of this research include extending a spatio-temporal model that accounts for spatial, temporal, and interaction effects, performing simulations to evaluate the model's effectiveness based on these trends, and measuring its performance by estimating parameters and assessing uncertainty. Additionally, the study aims to examine correlations and dependencies among random effects. It contributes significantly to Bayesian spatiotemporal analysis by introducing a hierarchical model that incorporates both spatial and temporal random effects with interaction terms. The parameters of the model are estimated using Gibbs sampling, and convergence diagnostics are applied to verify the model's accuracy in analyzing spatially and temporally varying phenomena.

METHODOLOGY

Spatio-Temporal Interaction Modelling

Spatial and temporal autocorrelations (random effects) were modeled via the conditional autoregressive (CAR) model proposed by [9] whose model can be expressed as

$$Y_{kt}|N_{kt},\theta_{kt}\sim Binomial(N_{kt},\theta_{kt}), \tag{1}$$

$$where \qquad \log(\frac{\theta_{kt}}{1-\theta_{kt}}) = X_{kt}^{T}\beta + \phi_k + \delta_t + \gamma_{kt}. \tag{2}$$

The proposed model is decomposed into the spatio-temporal random effects with 3 components as follows: where ϕ_k is the spatial effect, δ_t is the temporal effect and γ_{kt} is the set of spatio-temporal auto correlation random effect for the community k and time period t. $\theta_{kt} = Y_{kt}|N_{kt}$ is the proportion of children that having measles in space k at time t, for $k = 1,\cdots,k, t = 1,\cdots,N$ where the N_{kt} = 80, 160, 240, 320 and 400 respectively β is a vector of regression coefficients corresponding to covariates X. After adjusting for covariate effects, the first

component captures the overall spatial random effect common to all time period, represented by $\phi = (\phi_1, \phi_2, \cdots, \phi_n)$. The spatial relationships between communities in this study were shown by binary neighborhood matrices W.

$$\phi_k|\phi_{-kt}, W, \rho, \tau^2 \sim N\left(\frac{\rho_S \sum_{j=1}^{k} w_{kj}\phi_j}{\rho_S \sum_{j=1}^{k} w_{kj} + 1 - \rho_S}, \frac{\tau_S^2}{\rho_S \sum_{j=1}^{k} w_{kj} + 1 - \rho_S}\right). \quad (3)$$

The second part is a random effects in time that shows the overall trend in time that all communities share. This is shown by $\delta = (\delta_1, \delta_2, \cdots, \delta_n)$ where

$$\delta_t|\delta_{-t}, D \sim N\left(\frac{\rho_T \sum_{j=1}^{N} d_{tj}\delta_j}{\rho_T \sum_{j=1}^{N} d_{tj} + 1 - \rho_T}, \frac{\tau_T^2}{\rho_T \sum_{j=1}^{N} d_{tj} + 1 - \rho_T}\right). \quad (4)$$

In this study, temporal relationships between dependent variable were determined using an adjacency weights matrix, a binary $N \times N$, whrere $N = 1,2, \ldots, N$ temporal neighborhood matrix. $D = d_{tj}$ where $d_{tj} = 1$ is defined if $|j - t| = 1$ and $d_{ij} = 0$ otherwise.

The model can also include an optional set of independent space-time interactions, which are shown by $\gamma = (\gamma_1, \gamma_2, \ldots, \gamma_{nt})$ where

$$\gamma_{kt} \sim N(0, \tau_I^2). \quad (5)$$

and

$$\tau_S^2, \tau_T^2, \tau_I^2 \sim Inverse - Gamma(1, 0.001)$$

where $\tau_S^2, \tau_T^2, \tau_I^2$ represents random effects that can happen in spatial, temporal and space-time.

$$\rho_S, \rho_T \sim Uniform(0,1)$$

and ρ_S and ρ_T are spatial dependence parameters and temporal dependence parameters that control how strong spatial and temporal autocorrelations are.

SIMULATION STUDY

We conducted a simulation study to quantify the ability of the developed model to correctly assemble areas based on their temporal trends, spatial trend and interaction trend using the Gibbs

sampling approach. Data were simulated using Binomial logistic model, the model consist of the data likelihood $Y_{kt} \sim Binomial(n, \theta_{kt})$ where

$$\log(\frac{\theta_{kt}}{1-\theta_{kt}}) = \beta_0 + \beta_1 x_{1kt} + \beta_2 x_{2kt} + \phi_k + \delta_t + \gamma_{kt}$$

x_{1kt}, x_{2kt} are normally distributed covariate with mean 0 and variance 1, ϕ_k, δ_t, γ_{kt} corresponds to spatial and temporal that are drawn from multivariate normal distribution with mean vectors 0 and covariance structure defined as $\Sigma_K = 0.01Q_W^{-1}$, where W is the $K \times K$ distance matrix and $\Sigma_N = 0.01Q_D^{-1}$, where D is the $N \times N$ temporal matrix. The spatial-temporal covariance structures were simulated using

$$Q_W = 0.8\mathbf{I}_K\mathbf{1}'W - W + 0.2\mathbf{I}_K\mathbf{1}$$

for spatial effect

$$Q_D = 0.8\mathbf{I}_N\mathbf{1}'D - D + 0.2\mathbf{I}_N\mathbf{1}$$

for temporal effect.

This scheme implies that spatial and temporal correlations are set as $\rho_S, \rho_T = 0.8$ which also results in spatial, temporal and interaction effect defined by $\tau_S^2, \tau_T^2, \tau_I^2 = 0.2$. In addition, the intercept and covariate coefficients are defined as $\beta = (0,0.5,0.5)$ and $K = 16$ and $N = 5, 10, 15, 20$ and 25 areal units, $n_{kt} = N \times K = 80, 160, 240, 320$ and 400. Following, the simulation of the covariates and spatio-temporal effects and interaction, the response probability θ_{kt} were then simulated using

$$\theta_{kt} = \frac{\exp(\beta_0 + \beta_1 x_{1kt} + \beta_2 x_{2kt} + \phi_k + \delta_t + \gamma_{kt})}{1 + \exp(\beta_0 + \beta_1 x_{1kt} + \beta_2 x_{2kt} + \phi_k + \delta_t + \gamma_{kt})}.$$

The resoponse variable Y_{kt} was then generated from the $binomial(n_{kt}, \theta_{kt})$ distribution. The next step involve the application of the newly developed R function "binomial.est" to simulate the posterior distribution. The posterior distribution for the proposed model was obtained from 10,000 MCMC independent samples, which were generated from a single Markov Chain that was run for 120,000 iterations with a 20,000 burn-in period, subsequently thinned by 10 to reduce the autocorrelation of the Markov chain convergence and monitored using graphically Geweke diagnostic.

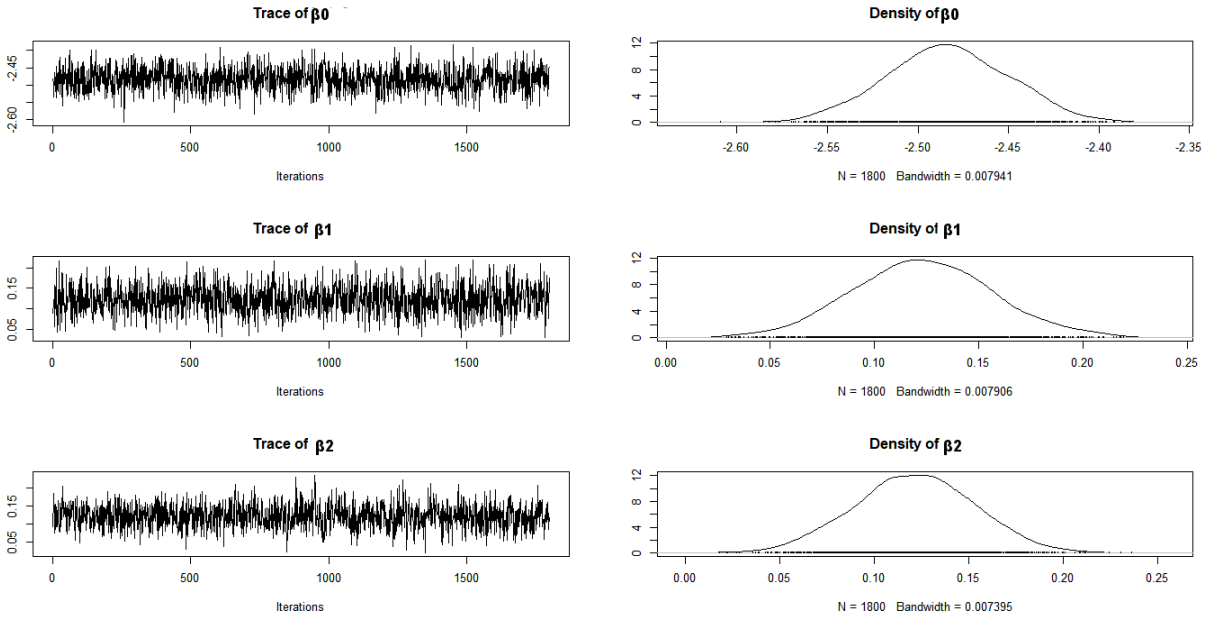

Figure 1: Trace and Density Plots for Estimated Parameters in MCMC Sampling (Areal Unit n_{kt}=80)

Figure 1: Trace and density plots for the areal unit with n_{kt}=80, K =16, n = 5 with true values $\beta_0 = 0, \beta_1 = 0.5, \beta_2 = 0.5$. The left panel illustrates the MCMC sample progress over iterations, while the right panel displays the posterior distribution of the parameters.

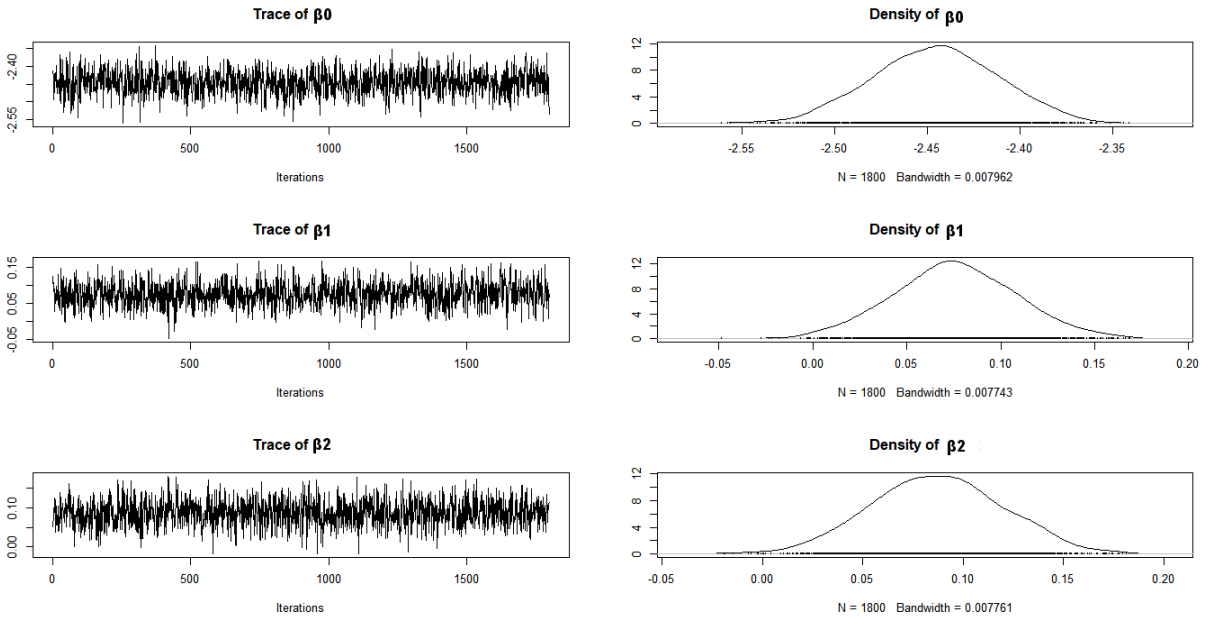

Figure 2: Trace and Density Plots for Estimated Parameters in MCMC Sampling (Areal Unit n_{kt}=160)

Figure 2: Trace and density plots for the areal unit with n_{kt}=160, K =16, n = 10 with true values $\beta_0 = 0, \beta_1 = 0.5, \beta_2 = 0.5$. The left panel illustrates the MCMC sample progress over iterations, while the right panel displays the posterior distribution of the parameters.

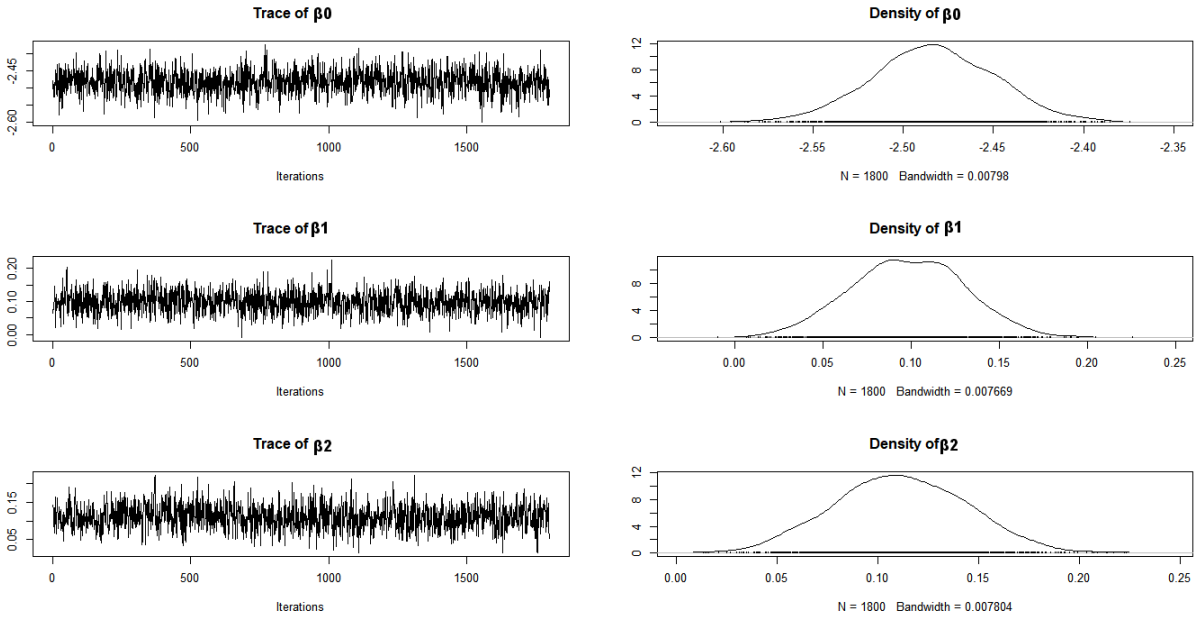

Figure 3: Trace and Density Plots for Estimated Parameters in MCMC Sampling (Areal Unit n_{kt}=240)

Figure 3: Trace and density plots for the areal unit with n_{kt}= 240, K =16, n =15 with true values $\beta_0 = 0, \beta_1 = 0.5, \beta_2 = 0.5$. The left panel illustrates the MCMC sample progress over iterations, while the right panel displays the posterior distribution of the parameters.

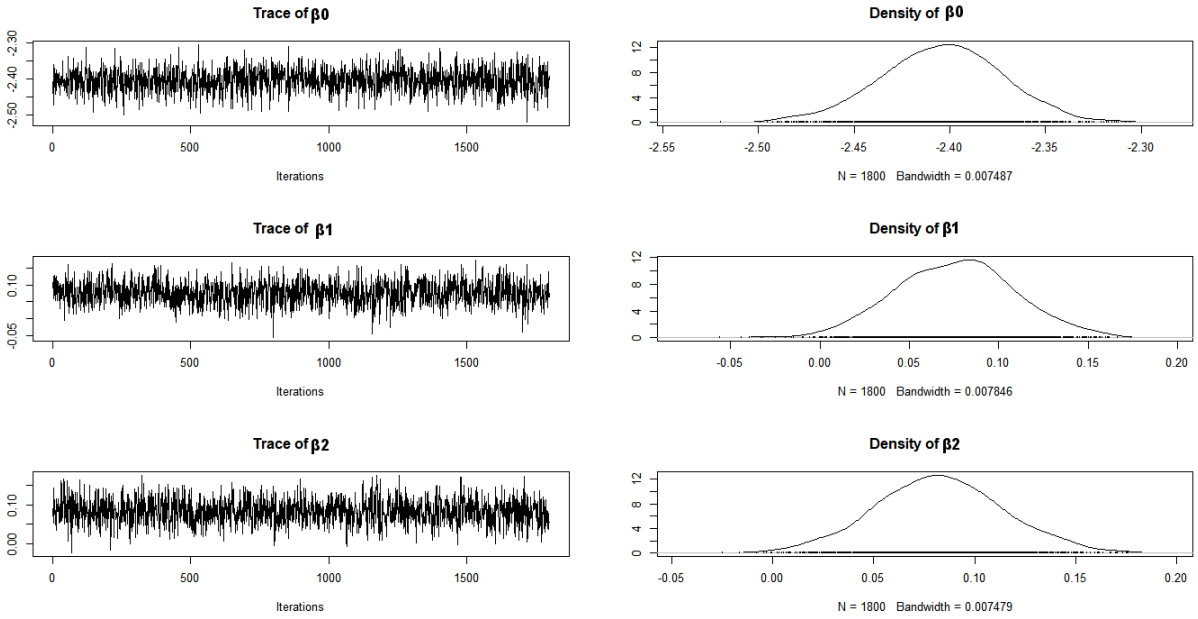

Figure 4: Trace and Density Plots for Estimated Parameters in MCMC Sampling (Areal Unit n_{kt}=320)

Figure 4: Trace and density plots for the areal unit with n_{kt}=320, K =16, n = 20 with true values $\beta_0 = 0, \beta_1 = 0.5, \beta_2 = 0.5$. The left panel illustrates the MCMC sample progress over iterations, while the right panel displays the posterior distribution of the parameters.

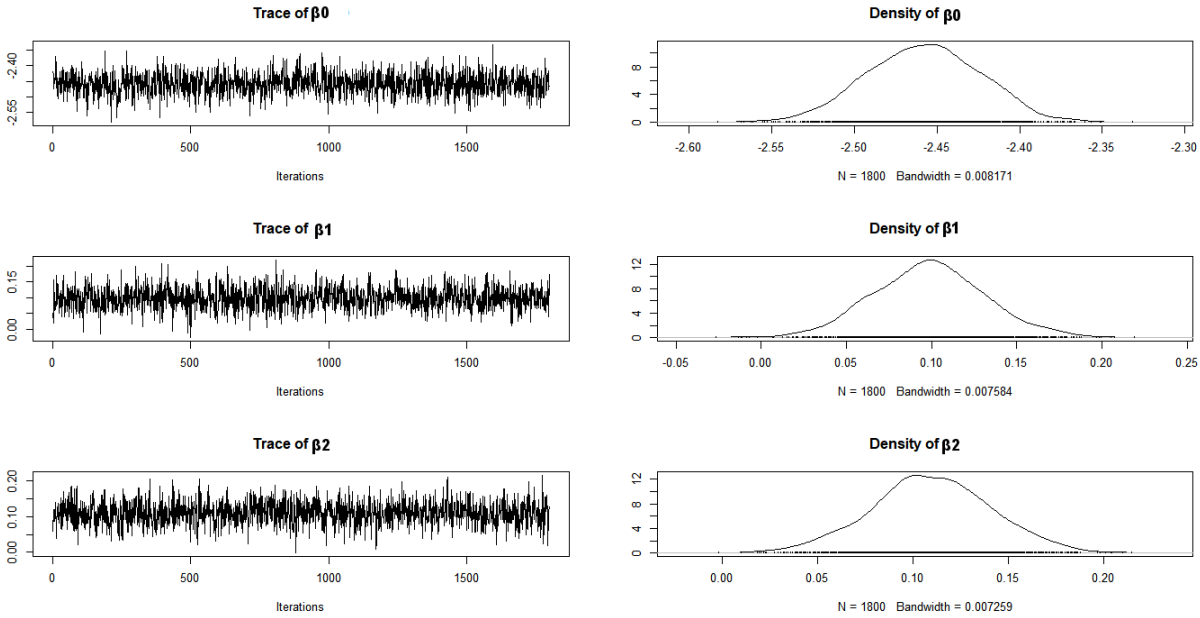

Figure 5: Trace and Density Plots for Estimated Parameters in MCMC Sampling (Areal Unit n_{kt}=400)

Figure 5: Trace and density plots for the areal unit with n_{kt}=400, K =16, n = 25 with true values $\beta_0 = 0, \beta_1 = 0.5, \beta_2 = 0.5$. The left panel illustrates the MCMC sample progress over iterations, while the right panel displays the posterior distribution of the parameters.

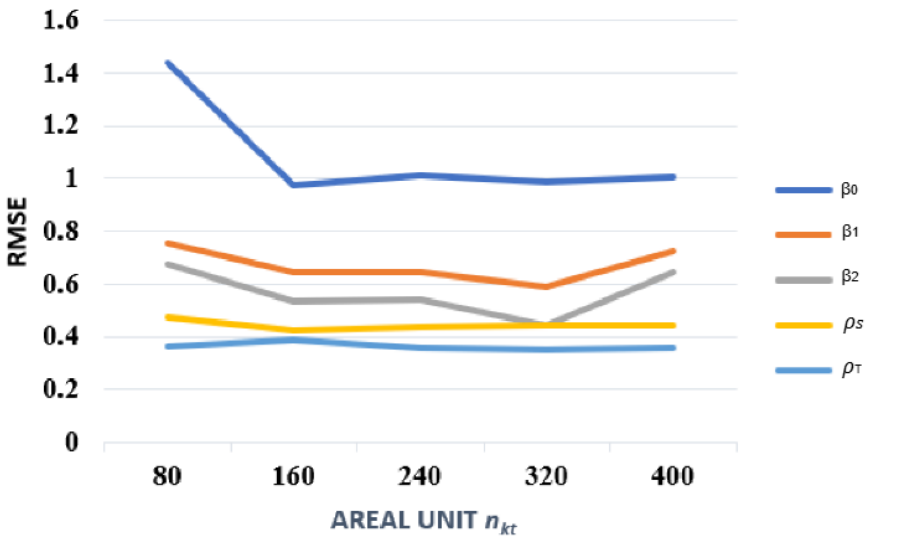

Figure 6: RMSE Across Different Areal Unit Sizes for β_0, β_1, β_2, τ_S, and τ_T

Figure 6: Graph showing RMSE values for β_0, β_1, β_2, τ_S, and τ_T across various areal unit sizes. The figure illustrates how RMSE for each parameter fluctuates with spatial scale, providing insights into the impact of areal unit size on model accuracy for different parameters.

Table 1: Posterior mean estimates and 95% credible intervals (C.I) for parameters β_0, β_1, β_2, τ_S, τ_T, τ_I, ρ_s and ρ_T across different areal units, n_{kt}= N * K= 80, 160, 240, 320, 400 with longitudinal value, K =16, and sample size N = 5,10,15,20, 25 and true parameter values $\beta_0 = 0$, $\beta_1 = 0.5$, $\beta_2 = 0.5$ and ρ_s=ρ_T=0.8

Areal Unit n_{kt}	Parameter	Mean estimate	95% C.I	S.E	RMSE	Geweke Z-test
80	β_0	-2.4864	(-2.5522, -2.4206)	0.0332	1.4398	1.4
	β_1	0.1228	(0.0562, 0.1887)	0.0319	0.7571	0.6
	β_2	0.0051	(0.0016, 0.0131)	0.0324	0.6779	-0.6
	ρ_S	0.4486	(0.0267, 0.9245)	0.2624	0.4740	0.5
	ρ_T	0.3998	(0.0165, 0.9083)	0.2587	0.3629	-0.8
	τ_S	0.0049	(0.0016, 0.0129)	0.0021	-	-0.9
	τ_T	0.0072	(0.0018, 0.0234)	0.0058	-	0.8
	τ_I	0.0037	(0.0013, 0.0086)	0.0023	-	-1.0
160	β_0	1.5708	(1.4037, 1.6223)	0.0564	0.9729	8.3
	β_1	0.5675	(0.4583, 0.6726)	0.0533	0.6461	2.4
	β_2	0.4822	(0.3773, 0.5842)	0.0546	0.5331	2.8
	ρ_S	0.4631	(0.0249, 0.9270)	0.2645	0.4259	-1.1
	ρ_T	0.3597	(0.0165, 0.8728)	0.2538	0.3908	0.1
	τ_S	0.0108	(0.0024, 0.0361)	0.0170	-	2.8
	τ_T	0.0093	(0.0019, 0.0325)	0.0064	-	-0.6
	τ_I	0.0620	(0.0028, 0.3209)	0.0425	-	0.8
240	β_0	1.5570	(1.4536, 1.6702)	0.0489	1.0093	0.3
	β_1	0.5314	(0.4428, 0.6219)	0.0450	0.6454	2.1
	β_2	0.5165	(0.4281, 0.6092)	0.0459	0.5433	-0.1
	ρ_S	0.4151	(0.0235, 0.9124)	0.2665	0.4396	-1.7
	ρ_T	0.4200	(0.0194, 0.9038)	0.2640	0.3587	-0.5
	τ_S	0.0158	(0.0021, 0.0768)	0.0098	-	0.9
	τ_T	0.0088	(0.0020, 0.0276)	0.0111	-	0.4
	τ_I	0.0310	(0.0159, 0.0542)	0.0554	-	-1.9
320	β_0	1.5344	(1.3893, 1.7163)	0.0830	0.9844	3.1
	β_1	0.5135	(0.4305, 0.6079)	0.0454	0.5889	-0.5
	β_2	0.5021	(0.4198, 0.5931)	0.0471	0.4401	2.4
	ρ_S	0.4151	(0.0181, 0.9005)	0.2634	0.4453	-0.3
	ρ_T	0.5523	(0.0429, 0.9619)	0.2634	0.3536	-0.8
	τ_S	0.0078	(0.0020, 0.0262)	0.0114	-	7.6
	τ_T	0.0233	(0.0040, 0.0708)	0.0049	-	1.2
	τ_I	0.0206	(0.0073, 0.0584)	0.2818	-	-0.6
400	β_0	1.5623	(1.4580, 1.7575)	0.0505	1.0005	37.2
	β_1	0.5097	(0.4364, 0.5985)	0.0347	0.7209	7.7
	β_2	0.5544	(0.4792, 0.6419)	0.0349	0.6421	13.6
	ρ_S	0.4097	(0.0157, 0.9185)	0.2667	0.4422	1.4

ρ_T	0.3733	(0.0112, 0.8685)	0.2375	0.3571	0.7
τ_S	0.0131	(0.0022, 0.0451)	0.0667	-	12.7
τ_T	0.0128	(0.0024, 0.0395)	0.0053	-	0.7
τ_I	0.1900	(0.0142, 0.8984)	0.1199	-	1.2

ANALYSIS AND DISCUSSION

The relationship between the log-odds of θ_{kt} and the predictors was expressed as $\frac{\ln(\theta_{kt})}{1-\theta_{kt}} = \beta_0 + \beta_1 x_{1kt} + \beta_2 x_{2kt}$. The regression coefficients were specified as $\boldsymbol{\beta} = (0,0.5,0.5)$.

To obtain the posterior distribution for our proposed model, we conducted Markov chain Monte Carlo (MCMC) sampling. 20,000 MCMC independent samples were generated from a single Markov chain and discarded the initial 2,000 samples as a burn-in period and thinned the remaining samples by 10 to reduce autocorrelation. Convergence of the MCMC chain was assessed using the Geweke diagnostic method, as well as graphical checking.

The MCMC sampling allowed us to obtain a posterior distribution that provided insights into the model's performance and the uncertainty associated with the estimated parameters.

The trace plots and the density plots for the estimated parameters $\hat{\beta}_0$, $\hat{\beta}_1$and $\hat{\beta}_2$ show that the density plots approximate a normal distribution, with average values falling between -2.4864, 0.1228 and 0.0051 for parameter values β_0, β_1 and β_2 respectively. The posterior estimate for the spatial and temporal autocorrelation, ρ_S and ρ_T are 0.4486 and 0.3998 with 95% credible intervals (0.0267, 0.9245) and (0.0165, 0.9083) respectively for the areal unit size of 80 and it was observed that the correlations values are positive correlation, the intercept, β_0 is -2.4864, with the 95% credible interval as (-2.5522, -2.4206), making the percent of baseline outcome close to -2.49 with fairly high accuracy. The main goal is to estimate the effects of the covariates; hence, Covariate 1 has a positive β_1, = 0. 1228 with the 95% credible interval of (0.0562, 0.1887) implying a small effect on the result was noted. Covariate 2, β_2 has a very low impact and it has a mean estimate of 0.0051 with 95% credible intervals of (0.0016, 0.0131). Therefore there's moderate level of spatial and temporal autocorrelation of the clusters but with high variability. The posterior correlation of the spatial, temporal and interaction random effects are τ_S, τ_T, τ_I are 0.0049, 0.0072 and 0.0037 with 95% credible intervals (0.0016, 0.0129), (0.0018, 0.0234) and (0.0013, 0.0086) respectively which indicated that there's a positive correlations, also considering the trace plots in Figure 1 for all the parameters, they shows that all the chains "wingled" and they overlap well, so the plots generated appear well and convergence is considered. Standard errors of these estimates vary from -1 to 1 as it can be seen from the Geweke Z-test values. 0 to 1. 4, meaning there is over all agreement, but some degree of variation.

Figure 2, displays the trace plots and the density plots for the estimated parameters β_0, β_1 and β_2. Additionally, as shown in Table 1, the size of the areal unit corresponds to the intercept, β_0 estimate for the areal unit size of 160 is 1.5708 with 95 % credible interval of (1.4037, 1.6223), purporting that the baseline outcome is around 1.57 with high precision. The coefficient of covariate 1 is large and positive at 0.5675 with C. I. of (0.4583, 0.6726), for which it can be seen that it has a strong positive relationship. Covariate 2, β_2 is equal to 0 with the mean estimate of the parameter 0.4822 with a credible interval of (0.3773, 0.5842), which reveals a significantly positive impact. The spatial and temporal autocorrelation, ρ_S and ρ_T are 0. 4631 and 0.3597 with 95% credible interval (0.0249, 0.9270) and (0.0165, 0.8728) proved the moderate spatial autocorrelation of the study area. Spatial variance, τ_S equals 0.0108, which is not very dissimilar among regions. Temporal variance, τ_T is slightly higher at 0 for gender and approximately 0. 0093,

interaction variance, τ_I is 0.0620. Geweke Z-test values range from -0. 6 to 2. 8 asserting that the majority of parameters have reached the corresponding values, while some of them indicate higher fluctuations.

When the areal unit size is 240, Figure 3 displays the trace and density plots for the estimated parameters, β_0, β_1 and β_2, as represented by the intercept, β_0 normal baseline outcome of 1.5570 with 95% credible intervals of (1.4536, 1.6702) reveal a stable baseline result. Covariate 1, β_1 is positively related with mean estimate of 0.5314 with corresponding 95% credib le intervals of (0.4428, 0.6219). Covariate 2, β_2 is estimated at the mean of 0.5165 with a credible interval of (0.4281, 0.6092) which indicates a positive correlation of the variable. The spatial an d temporal autocorrelation, ρ_S and ρ_T are 0.4151 and 0.4200 shows moderate spatial autocorrelation with 95% credible interval (0.0235, 0.9124) and (0.0194, 0.9038). Concerning the dispersion of spatial relationships, The posterior correlation of the spatial, temporal and interaction random effects are τ_S, τ_T, τ_I are 0.0131, 0.0128 and 0.1900 with 95% credible intervals (0.0022, 0.0451), (0.0024, 0.0395) and (0.0142, 0.8984) respectively which indicated that there's a positive correlations. The numbers of cell cycles per day for lobsters are 0.0131 and 0.0128, both quite close to each other indicating little variation. For Geweke Z-test values vary from -1. 9 to 0. 9 of which, revealed different levels of convergence of the parameters.

In the case of an areal unit size of 320, Figure 2 shows the trace and density plots for the estimated parameters, β_0, β_1 and β_2, the intercept was found to be 1.5344 represented by β_0 with a 95% credible interval of (1.3893, 1.7163), which showed that the baseline outcome has stabilised at 1.53. The coefficient for Covariate 1 is β_1 0.5135 with credible interval of (0.4305, 0.6079) which reveals positive impact. Estimate of Covariate 2 is β_2 with a mean estimate of 0.5021 with a 95% credible interval of (0.4198, 0.5931); showing a positive influence. The estim ate of the primary spatial and temporal auto-correlation coefficient, ρ_S and ρ_T are 0.4245 and 0.5523, with the 95% credible interval of (0.0181, 0. 9005) and (0.0429, 0.9619) Thus, the observed correlations among the random effects suggest a moderate level of spatial and temporal autocorrelations. The spatial variance, τ_S is 0.0078, indicating high spatial variability. In contrast, the temporal variance, τ_T is 0.0233, which suggests a lower level of temporal variability. The interaction variance, τ_I is 0.0206, indicating a moderate level of interaction between spatial and temporal effects with 95% credible interval (0.0020, 0.0262), (0.0040, 0.0708) and (0.0073, 0.0584) shows moderate interaction effects, all of which indicating that there's positive correlation. Geweke Z-test values vary from -0. 8 to 7. 6, for most of the parameters, the convergence is good as shown from the above results.

Similarly, for the areal unit size of 400, Figure 5 presents the trace and density plots for the estimated parameters β_0, β_1 and β_2, the intercept is estimated at 1 or β_0 1.5623 with a 95% credible interval of (1.4580, 1.7575), implying that the baseline outcome is about 1.56 with high precision. The estimate of Covariate 1, β_1 is equal to 0. All firm-specific controls were significant at the 5% level and positive in sign with mean values of 0.5097 with credible interval of (0.4364, 0.5985). On Covariate 2, β_2 the mean estimate is also equal to 0. As for the 95% credible interval values of the formula, they total 0.5544 with (0.4792, 0.6419) that, generally, indicate a positive impact. The specific spatial and temporal autocorrelation ρ_S and ρ_T are 0.4097 and 0.3733, with the 95% credible interval of (0.0157, 0. 9185) and (0.0112, 0.8685), and hence values suggesting moderate levels of spatial autocorrelation. Spatial variance, τ_S is equals 0.0131, reflecting moderate variability. Temporal variance, τ_T is 0.0128, and interaction variance, τ_I is 0.1900 respectively, and low variability, all of which indicating that there's positive correlation. The p-value based on the Geweke Z-test lie within the range of 0.7 to 37.2, which indicates fairly acceptable levels of convergence for most of the parameters used, although some of the individual parameters seem to be very high.

CONCLUSION

In this study, we extended Bayesian spatio-temporal models with space-time interaction effects. The simulation results indicated that the model effectively captured the relationship between covariates and health outcomes, with moderate spatial and temporal autocorrelations across the regions studied. Covariate 1 consistently played a significant role, while the overall variances indicated low to moderate variability in spatial and temporal effects.

The results demonstrated a good fit, suggesting that the model accurately reflects the relationship between the predictors and health outcomes in the longitudinal epidemiological data. Convergence diagnostics, including trace plots and the Geweke Z-test, further validated the model by confirming that the MCMC chains stabilized and produced reliable parameter estimates.

The RMSE analysis across different areal unit sizes indicates that the parameters β_0, β_1, and β_2 are influenced by spatial scale, with fluctuations showing higher sensitivity at smaller units. In contrast, the spatial correlation ρ_S and temporal correlation ρ_T remain relatively stable, suggesting that larger areal units yield consistent spatial and temporal dependencies. This stability implies that larger spatial scales may enhance the reliability of correlation estimates.

The insights gained from this analysis could contribute to a better understanding of spatial and temporal disease patterns, particularly in the epidemiology of infectious diseases like measles. These findings could also inform future public health interventions in regions susceptible to disease outbreaks.

REFERENCES

[1] Anderson, C., Lee, D. and Dean, N. (2016). Spatial clustering of average risks and risk trends in Bayesian disease mapping. Biometrical Journal, doi:201:10.1002/bimj.201600018.

[2] Bernardinelli, L., Clayton, D., Pascuto, C., Montomoli, C., Ghislandi, M. and Songini, M. (1995). Bayesian analysis of space-time variation in disease risk. Statistics in Medicine 14, 2433-2443.

[3] Cairns, K.L., Perry, R.T., Ryman, T.K., Nandy, R.K. & Grais, R.F. 2011. Should outbreak response immunization be recommended for measles outbreaks in middle- and lowincome countries? an update. The Journal of infectious diseases, 204(suppl_1):S35-S46.

[4] Choi, J., Lawson, A.B., Cai, B. and Hossain, M. (2011). Evaluation of Bayesian spatial-temporal latent models in small area health data. Environmetrics 22, 1008-1022.

[5] Charras-Garrido, M., Azizi, L., Forbes, F., Doyle, S., Peyrard, N. and Abrial, D. (2013). On the difficulty to delimit disease risk hot spots. Journal of Applied Earth Observation and Geoinformation 22, 99-105.

[6] Cressie, N. & Johannesson, G. Fixed rank kriging for very large spatial data sets. Journal of the Royal Statistical Society. *Series B (Statistical Methodology)*. **70**, 209-229 (2008)

[7] Gelfand, A. E., Diggle, P. J., Guttorp, P., & Fuentes, M. (Eds.). (2010). Handbook of spatial statistics. CRC press.

[8] Geweke J. Evaluating the accuracy of sampling-based approaches to the calculation of posterior moments. In: Bernardo JM, Berger JO, Dawid AP, et al. (eds) Bayesian statistics. Oxford: University Press, 1992, pp.169-193.

[9] Haining, R. P., and Li, G. (2020). Regression Modelling With Spatial and Spatial-Temporal Data: A Bayesian Approach. CRC Press.